Combined mineralogy and chemistry on drill cores: challenging for on-line-real-time analyses

Cédric Duée, Nicolas Maubec, Valérie Laperche, Laure Capar, Anne Bourguignon, Xavier Bourrat
BRGM

Yassine El Mendili, Daniel Chateigner, Stéphanie Gascoin
Normandie Université, CRISMAT-ENSICAEN, UMR CNRS 6508

Gino Mariotto, Marco Giarola, Arun Kumar, Nicola Daldosso, Marco Zanatta, Adolfo Speghini
University of Verona

Andrea Sanson
University of Padua

Luca Lutterotti, Evgeny Borovin, Mauro Bortolotti, Maria Secchi, Maurizio Montagna
University of Trento

Beate Orberger*, Monique Le Guen, Anne Salaün, Céline Rodriguez, Fabien Trotet, Mohamed Kadar, Karen Devaux
*ERAMET-RESEARCH-SLN *and: GEOPS, Université Paris Sud, Université Paris Saclay*

Henry Pillière, Thomas Lefèvre
Thermo Fisher Scientific

Fons Eijkelkamp, Harm Nolte, Peter Koert
Royal Eijkelkamp

Saulius Grazulis
Vilnius University Institute of Biotechnology

Abstract. In order to evaluate the instrumental parameters for the combined on-line-on-mine-real-time expert system SOLSA (http://www.solsa-mining.eu), portable and laboratory analyses were carried out on coarse granite, sandstone, serpentinized harzburgite and siliceous breccia. Each sample was studied at 5 different surface roughnesses (sonic or diamond drilled, cut, polished at 6 µm and 0.25 µm, sample powders). X-ray diffraction (XRD), portable Infra-Red (pIR) and X-ray-fluorescence (pXRF), and laboratory micro-Raman spectroscopy gave complementary and corroborating results. No major effect on the analyses was noted for the selected surface states. pXRF gave variable results except for the homogeneously serpentinized harzburgite, related to coarse or contrasting grain sizes or pores, small spot size (3 mm) and needs close-to-surface analyses. Portable IR (spot size 1.76 cm^2) is carried out close to surfaces while Raman spectroscopy (1-2 µm) is performed at distance. Sampling strategies have to be defined for each lithology. Major challenges for a combined on-line analysis are to adapt the specificities of the techniques to (1) analyse similar surface areas (from ~2 cm^2 (pIR) to < µm (Raman)), (2) smartly combine all the techniques into a single instrument, and (3) develop appropriate databases to reach a reliable "real-time" outcome results, which can be used for more precise geomodeling, and to rapidly define exploration and beneficiation parameters.

1 Introduction

Combined mineralogical and chemical analyses on drill cores are highly demanded by mining and metallurgical companies to speed up exploration, mining and define geometallurgical parameters for beneficiation. At present, analyses are done by exploiting only a single technique, such as hyperspectral imaging, XRF or LIBS (Cudahy et al. 2009; Roache et al. 2011; Haest et al. 2012). The coupling of different analytical instruments is still a technological challenge. The SOLSA project, sponsored by the EU-H2020 Raw Material program, targets to construct an expert system coupling sonic drilling with XRF, XRD, hyperspectral imaging and Raman spectroscopy. In order to define optimal instrumental parameters for combined on-line-real-time-on-mine analyses, we probed sonic and diamond drill core materials from sedimentary, magmatic and hydrothermally altered rock as well as sample powders (Fig. 1 a-e) by a cross-method approach.

2 Sample material and analytical methods

Sonic and diamond drilled core parts were cut from the core material (20 mm^2 x 6 mm). Four types of surface conditions were studied: (a) convex surface as drilled, (b) diamond saw-cut, (c) polished at 6 µm, (d) polished at 0.25 µm and (e) powdered at < 80 µm (Fig 2). Multiple measurements (pIR, pXRF, Raman spectroscopy) were carried out on each surface of the 4 surface states on coarse sandstone, coarse granite, porous breccia and serpentinized harzburgite, in order to evaluate the effects of the surface roughness on the different techniques.

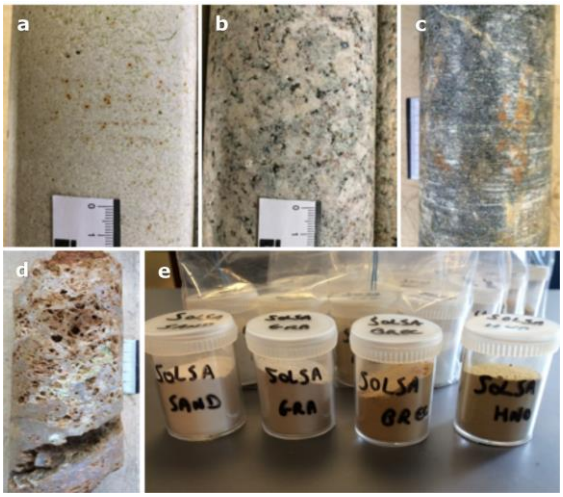

Figure 1. Sonic drilled cores (Royal Eijkelkamp, NL) of sandstone (**a**), and granite (**b**); diamond drilled cores (SLN, NC) of serpentinized harzburgite (**c**) and breccia (**d**); **e**: powdered samples (< 80 µm) of the abovementioned sample materials.

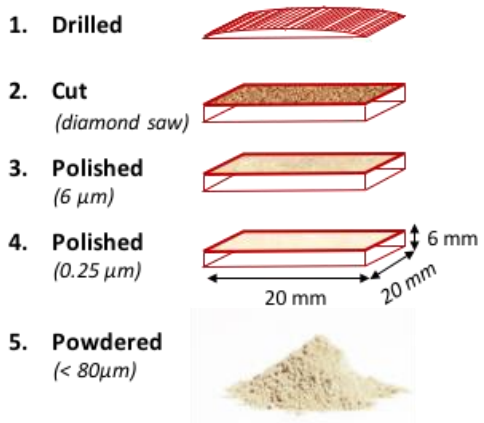

Figure 2. Sketch of the sample preparation for the surface roughness analyses.

Handeld X-ray fluorescence (pXRF) analyses were performed by Thermo Fisher NITON XL3t 980 (BRGM & ERAMET-COMILOG, 120 s acquisition time, 4 filters, mining mode, diameter of the analytical window: 0.3 cm). Five measurements were acquired on different zones of each sample type. Handheld infra-red spectroscopy (pIR) was carried with an ASD FieldSpec 3 (BRGM, band width: 350 to 2500 nm, 3-10 nm spectral resolution, area of the analytical window 1.76 cm^2). For each sample, 10 spectra (=20 measurements: 1/10 s) were compared in order to ensure the absence of aberration, and summed to obtain the final reflectance spectrum. Micro-Raman spectroscopy was performed with Jobin-Yvon LabRam HR800 (University of Verona; 633 nm He-Ne laser, powers at the sample surface: 1.5, 3 and 6 mW, spot size 1-2 µm, and integration time 20 s and 100 s), and with ThermoScientific DXR (CRISMAT-ENSICAEN, 532 nm laser, power at the sample surface: 1 mW, spot size 0.6 µm, and integration time of 120 s). XRD was carried out on powdered samples with a Siemens D5000 diffractometer (BRGM; Co-tube, 2θ range from 4° to 84°, with 0.03° step and 13.5 s/point). DIFFRAC Plus EVA software was used for the interpretation of the X-ray diffraction patterns. Quantitative mineralogy was estimated using Rietveld refinement and MAUD software.

3 Results

Peridotite. XRD powder analysis shows 57 wt.% serpentine, 29 wt.% forsterite, 11 wt.% enstatite, 3 wt.% talc and traces of amphibole (Fig. 3). pIR on dark green peridotite shows weak reflectance and detects serpentine. Polishing may decrease the reflectance and slightly enhance the peak intensity (Fig. 4). Micro-Raman spectroscopy precises that the major serpentine mineral is lizardite, confirms the presence of both forsterite and enstatite, and, additionally, detects quartz, anatase, rutile, pyrite, magnetite, maghemite and goethite (Fig. 5). pXRF analyses on the powder surface indicate 21.9 ± 0.2 wt.% Si, 20.6 ± 0.9 wt.% Mg, 5.9 ± 0.1 wt.% Fe, 88 ± 7 ppm V, 39 ± 1 ppm Ti, 2194 ± 43 ppm Ni, 1417 ± 119 ppm Cr, 40 ± 5 ppm Zn and 896 ± 45 ppm Mn. Analyses on the drilled, cut and polished surfaces show higher values for Si (22.8-24.2 wt.%), Mg (23.1-26.1 wt.%) and Ti (41-63 ppm), similar contents of Fe, Ni, Zn, Mn, and variable contents of V and Cr compared to those on the powdered sample.

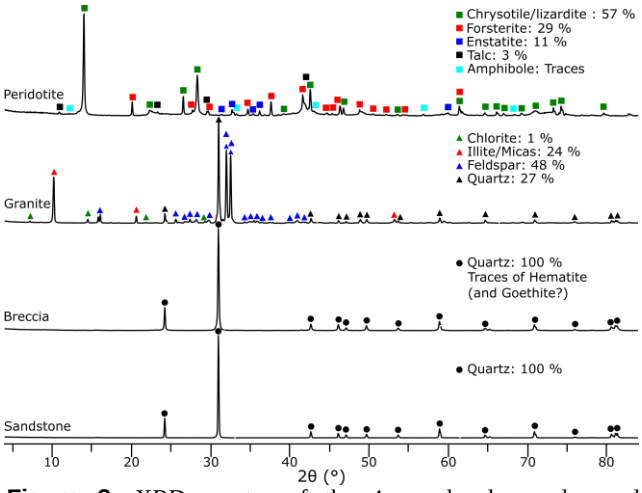

Figure 3. XRD spectra of the 4 powdered samples and quantitative estimations (Rietveld refinement-MAUD software).

Granite. XRD powder analysis shows a composition of 27 wt.% quartz, 20 wt.% microcline, 28 wt.% albite, 24 wt.% mica and/or illite and 1 wt.% chlorite. pIR shows the presence of bound water and illite, in agreement with XRD analyses. Micro-Raman spectroscopy confirms the presence of quartz, albite, precises the presence of muscovite and detects additionally gypsum, magnesium sulphate, rutile, anatase, calcite and hematite (Fig. 5). pXRF on powder surface indicates 39.3 ± 0.4 wt.% Si, 9.2 ± 0.2 wt.% Al, 0.6 ± 0.1 wt.% Ca, 4.2 ± 0.1 wt.% K, 95 ± 13 ppm Zr, 59 ± 1 ppm Sr, 301 ± 39 ppm Ba, 43 ± 7 ppm Zn, 38 ± 4 ppm Pb, 0.9 ± 0.1 wt.% Fe, 136 ± 10 ppm V, 961 ± 64 ppm Ti and Ni and Cr below the detection limits. Analyses on drilled, cut and polished surfaces show higher

Si contents (42-46 wt.%), and variable contents of the other elements. Cr was detected on polished surfaces (235–324 ppm). These heterogeneous results are due to the coarse grain size of the granite.

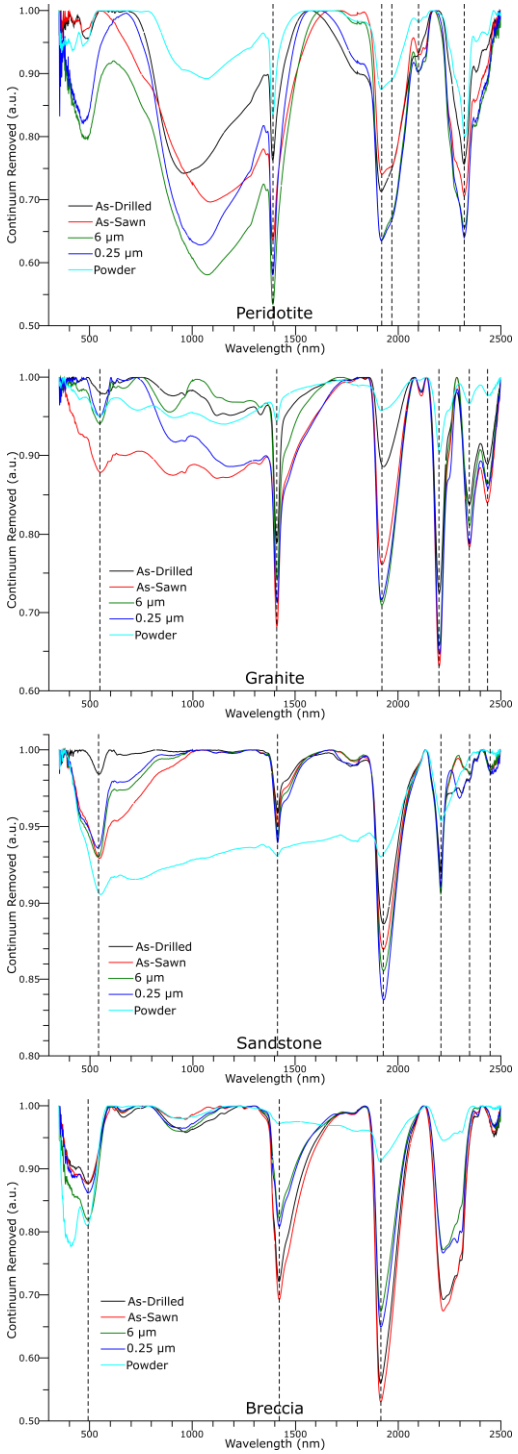

Figure 4. Portable hyperspectral spectra on the 5 different surfaces (as drilled, as cut, polished 6 µm and 0.25 µm, and powder surface).

Sandstone. XRD powder analysis shows a composition of 100 wt.% quartz (Fig. 3). pIR analyses on the powdered samples give generally higher reflectance than the analyses on the drilled, cut or polished surfaces. Polishing slightly decreases the reflectance and slightly increases the peak intensity. pIR indicates the presence of bound water and illite or montmorillonite (Fig. 4). Micro-Raman spectroscopy confirms the presence of quartz and detects anatase, pyrite, maghemite, goethite and zircon. pXRF on the powder shows 55.2 ± 0.5 wt.% Si, 132 ± 16 ppm Zr, 0.02 ± 0.01 wt.% Fe, 55 ± 6 ppm V, 358 ± 59 ppm Ti, 0.05 ± 0.01 wt.% K, and 0.01 ± 0.01 wt.% Ca. Analyses on the drilled, cut and polished surfaces are lower in particular for the trace elements Zr (50-100 ppm) and Ti (99-256 ppm), Fe is heterogeneously distributed (260-600 ppm). From the chemical analyses, it can be concluded that minor amounts of zircons, iron oxi-hydroxides and Ti-oxides are present. This is confirmed by Raman spectroscopy. The traces of illite are indicated by traces of K, the traces of Ca may be related to carbonates.

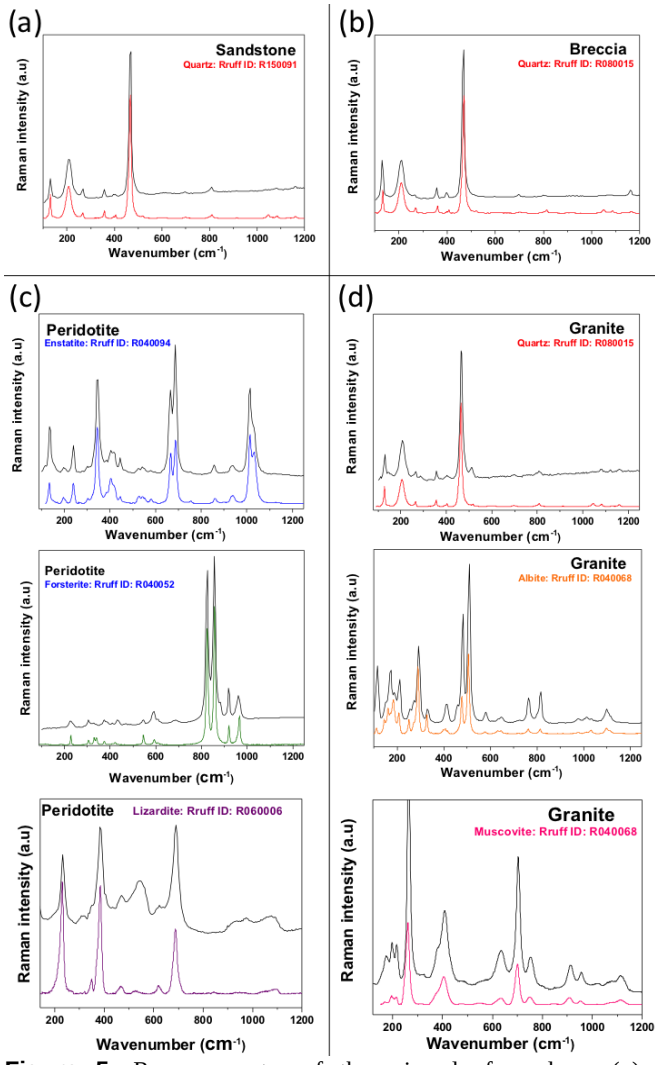

Figure 5. Raman spectra of the minerals formed on (**a**) Sandstone (**b**) Breccia (**c**) Peridotite and (**d**) Granite. All spectra are compared to those presented in RRUFF Raman database http://rruff.info.

Breccia. According to XRD powder analyses, the sample contains 100 wt.% of quartz with traces of hematite

and goethite (Fig. 3). pIR spectra do not allow to identify quartz, as the latter is detected around 9000 nm (TIR region). Water molecules are identified at 1420 and 1920 nm. The 500 nm band may correspond to goethite (Fig. 4). Micro-Raman spectroscopy confirms quartz as the major phase, and the presence of hematite and goethite. Furthermore, hedenbergite, forsterite, calcite, magnetite and maghemite were detected (Fig. 5). pXRF on the breccia powder indicates 53.5 ± 0.2 wt.% Si, 1.7 ± 0.1 wt.% Fe, 3722 ± 59 ppm Ni and 786 ± 57 ppm Cr. Sawn surfaces give lowest trace element values. As for sandstone, analyses on the drilled, cut and polished surfaces generally results into lower and highly variable concentrations (241-1520 ppm Ni; 12 ppm–1.2 wt.% Fe, 86-480 ppm Cr). Ni and Fe are positively correlated, indicating a common phase. Cr traces may reflect chromite, as Cr is not correlated to Ni or Fe. Raman analyses give important arguments (1) that the breccia is an alteration product of harzburgites; (2) the redox-conditions of breccia formation.

4 Discussion and conclusions

Lithology	Mineralogy				Chemistry		
		XRD	Raman	pIR	pXFR		
	Spot Size	Powder	0.6-2 µm	1.76 cm²	3 mm (powder)		
		wt.%			Elements	Concentration	
Serpentinized Harzburgite (Peridotite)	*Serpentine*	57	Lizardite	xx			
	Forsterite	29	xx		Si	21.9 ± 0.2	wt.%
	Enstatite	11	xx		Mg	20.6 ± 0.9	
	Talc	3			Fe	5.9 ± 0.1	
	Amphibole	traces					
	Quartz		x		V	88 ± 7	ppm
	Anatase		x		Ti	39 ± 1	
	Rutile		x		Ni	2194 ± 43	
	Pyrite		x		Cr	1417 ± 119	
	Magnetite		x		Zn	40 ± 5	
	Maghemite		x		Mn	896 ± 45	
	Goethite		x				
Coarse Granite	*Quartz*	27	xx		Si	39.3 ± 0.4	wt.%
	Microcline	20			Al	9.2 ± 0.2	
	Albite	28	xx		Ca	0.6 ± 0.1	
	Mica/Illite	24	Muscovite/Illite	Illite	K	4.2 ± 0.1	
	Chlorite	1	x		Fe	0.9 ± 0.1	
	Gypsum		x		V	136 ± 10	ppm
	Mg Sulfate		x		Ti	961 ± 64	
	Rutile		x		Zr	95 ± 13	
	Anatase		x		Ba	301 ± 39	
	Calcite		x		Sr	59 ± 1	
	Hematite		x		Zn	43 ± 7	
	Bound Water			x	Pb	38 ± 4	
Sandstone	*Quartz*	100	xx		Si	55.2 ± 0.5	wt.%
	Illite/Montmorillonite			x	Fe	0.02 ± 0.01	
	Anatase		x		Ca	0.01 ± 0.01	
	Pyrite		x		K	0.05 ± 0.01	
	Maghemite		x				
	Goethite		x		V	55 ± 6	ppm
	Zircon		x		Ti	358 ± 59	
	Bound Water			x	Zr	132 ± 16	
Siliceous Breccia	*Quartz*	100	xx				
	Hematite	traces	x				
	Goethite	traces	x	x	Si	53.5 ± 0.2	wt%
	Hedenbergite		x		Fe	1.7 ± 0.1	
	Forsterite		x				
	Calcite		x		Ni	3722 ± 59	ppm
	Magnetite		x		Cr	786 ± 57	
	Maghemite		x				
	Bound Water			x			

XRD (with Rietveld refinment) and Raman spectroscopy are performed with laboratory equipments

pIR and pXRF are performed with portable equipments

pXRF values are averaged and rounded (5 analyses/sample)

Table 1. Summary of major results of the combined sensor analyses on the 4 lithologies and 5 surface states.

This study shows how, in heterogeneous coarse grained and porous materials, a multi-technique approach is needed to obtain reliable chemical and mineralogical characterization. Table 1 summarises the results of combined portable sensors and laboratory instruments. Moreover, the presented data show that different surface treatments on the same sample have only minor effects on XRD, micro-Raman, pIR and pXRF measurements.

At present, a multi-technique approach is time consuming and requires different laboratory apparatuses. In order to integrate XRD, XRF, micro-Raman, and IR on a single probe operating at on-line-on-mine conditions there are some major technical challenges including (1) the adaption of powerful laboratory XRD and Raman spectrometers to a compact on-line-on-mine instrument; (2) the adaption and robotisation of the combined sensor system to overcome the problem of the different spot sizes from cm (IR) to mm (XRF) down to micrometric scales (Raman spectroscopy).

Finally, a reliable analysis cannot leave out of consideration the development of a mineral library adequate to the specific characteristics of the ore and waste to be analysed. This database should be comprehensive for Raman, XRD and hyperspectral data.

Acknowledgements

The SOLSA Consortium thanks the European Commission for having sponsored this project SC5-11d-689868 in the H2020 program: SC5-11d-689868.

References

Cudahy T, Hewson R, Caccetta M, Roache A, Whitbourn L, Connor P, Coward D, Mason P, Yang K, Huntington J, Quigley M (2009) Drill core logging of plagioclase feldspar composition and other minerals associated with Archean gold mineralization at Kambalda, Western Australia, using a bidirectional thermal infrared reflectance system. Reviews in Economic Geology 16:223-235.

Haest M, Cudahy T, Laukamp C, Gregory S (2012) Quantitative Mineralogy from Infrared Spectroscopic Data. I. Validation of Mineral Abundance and Composition Scripts at the Rocklea Channel Iron Deposit in Western Australia. Economic Geology 107:209-228.

Roache TJ, Walshe JL, Huntington JF, Quigley MA, Yang K, Bil BW, Blake KL, Hyvärinen T (2011) Epidote–clinozoisite as a hyperspectral tool in exploration for Archean gold. Australian Journal of Earth Sciences 58:813-822. doi: 10.1080/08120099.2011.608170.